



**NIST Technical Note  
NIST TN 2342**

# **Measurement and Uncertainty Analysis of Pressure Losses in Push-to-Connect Elbows and Couplings**

Lingnan Lin  
Natascha Milesi Ferretti  
Glen Glaeser  
Kyu Young Kim

This publication is available free of charge from:  
<https://doi.org/10.6028/NIST.TN.2342>

**NIST Technical Note  
NIST TN 2342**

# **Measurement and Uncertainty Analysis of Pressure Losses in Push-to-Connect Elbows and Couplings**

Lingnan Lin<sup>1,2</sup>, Natascha Milesi Ferretti<sup>3</sup>, Glen Glaeser<sup>3</sup>, Kyu Young Kim<sup>4</sup>

<sup>1</sup> *Department of Mechanical Engineering  
University of Maryland, College Park*

<sup>2</sup> *PREP Associate, Building Energy and Environment Division  
Engineering Laboratory, NIST*

<sup>3</sup> *Building Energy and Environment Division  
Engineering Laboratory, NIST*

<sup>4</sup> *LG Electronics  
Seoul, Republic of Korea*

This publication is available free of charge from:  
<https://doi.org/10.6028/NIST.TN.2294>

July 2025



U.S. Department of Commerce  
*Howard Lutnick, Secretary*

National Institute of Standards and Technology  
*Craig Burkhardt, Acting NIST Director and Deputy Under Secretary of Commerce for Standards and Technology*

NIST TN 2342  
July 2025

Certain commercial equipment, instruments, software, or materials, commercial or non-commercial, are identified in this paper in order to specify the experimental procedure adequately. Such identification does not imply recommendation or endorsement of any product or service by NIST, nor does it imply that the materials or equipment identified are necessarily the best available for the purpose.

### **NIST Technical Series Policies**

[Copyright, Use, and Licensing Statements](#)

[NIST Technical Series Publication Identifier Syntax](#)

### **Publication History**

Approved by the NIST Editorial Review Board on 2025-06-23

### **How to Cite this NIST Technical Series Publication**

Lin, L., Milesi-Ferretti, N., Glaeser, G., Kim, K. Y. (2025) Measurement and Uncertainty Analysis of Pressure Losses in Push-to-Connect Elbow and Coupling. (National Institute of Standards and Technology, Gaithersburg, MD), NIST Technical Note (TN) NIST TN 2342. <https://doi.org/10.6028/NIST.TN.2342>

### **NIST Author ORCID iDs**

Lingnan Lin: 0000-0002-0813-7613

Natascha Milesi Ferretti: 0009-0007-7273-0925

Glen Glaeser: 0009-0007-9383-5224

### **Contact Information**

[natascha.milesi-ferretti@nist.gov](mailto:natascha.milesi-ferretti@nist.gov)

## Abstract

Pressure losses in pipe fittings are essential to sizing plumbing systems, yet most existing data are outdated and not applicable to modern plumbing fittings. This paper presents the measurements of pressure losses for two push-to-connect fittings (a coupling and an elbow) that are widely used in modern plumbing systems. Both fittings are commercially available, made of lead-free brass, and have a nominal tube size (NTS) of  $\frac{3}{4}$ . The pressure loss was determined by measuring the pressure distribution upstream and downstream of the fitting, from which hydraulic grade lines were established. The tests were conducted for flow velocities from 0.6 m/s to 4.6 m/s, covering the typical conditions in premise plumbing. The corresponding Reynolds number ( $Re$ ) ranges from approximately  $10^4$  to  $10^5$ . The results show that the pressure loss coefficient of the elbow decreases with  $Re$  before leveling off at 1.0 when  $Re$  exceeds 40000. In contrast, the pressure loss coefficient of the coupling is independent of  $Re$ , with an average value of 0.007. Equivalent lengths—another parameter commonly used in plumbing industry to characterize pressure loss—are also reported. The equivalent length of the elbow ranges between (0.8 to 1.1) m for the tested range of  $Re$ , while that of the coupling ranges between (4.5 to 7.5) mm. Another key finding related to the development of standard testing procedures is that additional tapping locations upstream can reduce the uncertainty associated with the pressure loss measurement. Increasing the upstream tapping locations from three to five can result in a reduction of the expanded uncertainty by up to 75 %.

## Keywords

Pressure, Flow, Water, Fittings, Plumbing, Coupling, Elbow

## Table of Contents

<b>1. Introduction</b> .....	<b>1</b>
<b>2. Test Facility and Test Method</b> .....	<b>1</b>
<b>3. Test Fittings</b> .....	<b>4</b>
<b>4. Calculation of Measurement Uncertainty</b> .....	<b>5</b>
4.1. Uncertainty of Primary Measurements .....	5
4.2. Uncertainty of Pressure Loss .....	6
4.3. Uncertainty of Velocity .....	7
4.4. Uncertainties of Pressure Loss Coefficient, $K_L$ .....	8
<b>5. Measurement Data and Analysis</b> .....	<b>9</b>
5.1. Elbow.....	9
5.2. Coupling .....	12
<b>6. Conclusions</b> .....	<b>13</b>
<b>References</b> .....	<b>14</b>
<b>Appendix A. Test Data and Uncertainties</b> .....	<b>15</b>
<b>Appendix B. Equivalent Length vs. Volumetric Flow Rate in English Units</b> .....	<b>18</b>

## List of Tables

Table 1. Pressure tapping locations in the test section.....	2
Table 2. Uncertainties of primary measurements .....	6
Table A1. Uncertainties of elbow pressure losses .....	15
Table A2. Uncertainties of the elbow's pressure loss coefficient and its components.....	16
Table A3. Uncertainties of coupling pressure losses .....	17
Table A4. Uncertainties of the coupling's pressure loss coefficient and its components .....	17

## List of Figures

Figure 1. Schematic of the test facility.....	2
Figure 2. Schematic of the test section and pressure measurement system. ....	3
Figure 3. Dimensions of the test elbow and coupling .....	5
Figure 4. Pressure loss coefficient of elbow as a function of Re.....	9
Figure 5. Pressure distribution for Test 3 of elbow at (a) 0.6 m/s (2 ft/s), (b) 1.5 m/s (5 ft/s), and (c) 4.6 m/s (15 ft/s).....	11
Figure 6. Friction factor ( $f$ ) of the straight pipes upstream and downstream of the elbow (Test 3). .....	12
Figure 7. Equivalent length of the elbow as a function of Re. ....	12
Figure 8. Pressure loss coefficient of the coupling as a function of Re .....	13
Figure 9. Equivalent length of the coupling as a function of Re calculated from the mean $K_L$ of coupling .....	13

## **Acknowledgments**

The authors gratefully acknowledge Weiheng Oh of the Rensselaer Polytechnic Institute for his analytical and experimental works during his summer internships at NIST, and Tania Ullah, Dan Cole, and Lisa Ng for their review and suggestions on the manuscript. The author L. Lin was supported by the NIST Professional Research Experience Program (PREP) (Award Number: 0002525).

## 1. Introduction

Pressure losses in fittings are critical to sizing a plumbing system. Incorrect sizing can hinder achieving desired flow rates, increase installation and operational cost, and reduce energy efficiency. In premise plumbing systems, oversized pipes can also result in increased water age and lower disinfectant residuals, fostering conditions favorable for the growth of opportunistic pathogens such as *Legionella pneumophila* [1].

Currently, the pressure loss data published in engineering handbooks of refs [2–6] are most widely used. However, as found in our recent literature survey [7], the majority of these data originate from outdated studies where the fittings were made of now-obsolete material or geometric design. Large errors are commonly expected when using these data for today's plumbing fittings. In addition to lacking updated data, there remains no standard method in the plumbing industry to test fittings for pressure loss. Therefore, the Building Energy and Environment Division at NIST launched a project aiming to develop a pressure loss test method and provide updated data for modern plumbing fittings. A new test facility was built in 2023, as described in a previous report [8]. This report presents the first batch of data collected in the new test facility for an elbow and a coupling, both are copper and push-to-connect. In addition, this report provides an extensive uncertainty analysis as well as lessons learned and suggestions for future modification on the method and apparatus.

## 2. Test Facility and Test Method

Figure 1 shows the schematic of the test facility. The test facility comprises of a closed water loop driven by a variable-speed centrifugal pump. The test section consisted of a 1.5 m upstream tube, the test fitting, and a 2.1 m downstream tube. The two pipes were cut from the same NTS  $\frac{3}{4}$ , Type L copper tube, with an inside diameter of 20.11 mm (0.791 in), measured using a vernier caliper. A flow conditioner was installed before the test section to reduce the length needed to establish fully-developed flow. Three Coriolis flow meters were used to measure the density and mass flow rate. The water temperature was measured using three PT100 resistance temperature detectors (RTDs) placed near the inlet and outlet of the test section. More details about the test facility and test method are found in our previous publication [8].

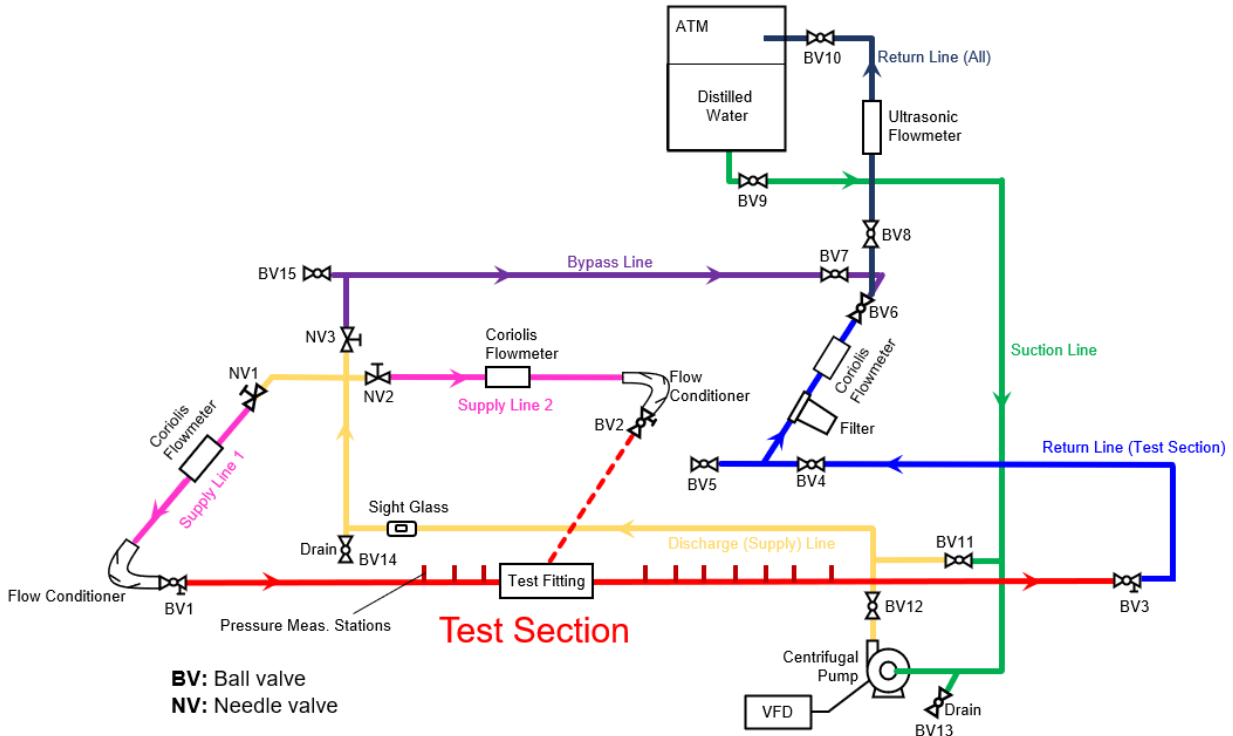


Figure 1. Schematic of the test facility

The test section had ten pressure measurement stations along the pipe, including three upstream and seven downstream of the fitting, as shown in Figure 2. Their streamwise locations are listed in Table 1. As will be shown in Section 5, the flow at these locations was fully developed. At each location, four 1.57-mm (i.e., 1/16-inch) taps were uniformly spaced around the circumference of the pipe, and inter-connected via a custom designed piezometer ring [8]. The pressure taps were bored using an end mill to ensure that the holes were perpendicular to the wall and that the edges of the holes were square with the wall surface and free from any burrs or irregularities.

Table 1. Pressure tapping locations in the test section

Number	Type	Location, $z$ [m]*	Location, $z$ [Diameter] *
1	Upstream	-0.4572	-24
2	Upstream	-0.2667	-14
3	Upstream	-0.0762	-4
4	Downstream	0.3810	20
5	Downstream	0.5715	30
6	Downstream	0.7620	40
7	Downstream	0.9525	50
8	Downstream	1.1430	60
9	Downstream	1.3335	70
10	Downstream	1.7145	90

\* Locations are relative to the fitting (i.e., at the fitting,  $z = 0$ )

These pressure measurement stations are part of an automated pressure measurement system was devised to measure the static pressures with high accuracy (reported in Section 4) for a wide

range of conditions. It included five sets of differential pressure (DP) transducers with different ranges, dividing the entire range into five bins: < 2.5 kPa, (2.5 to 6.9) kPa, (6.9 to 13.8) kPa, (13.8 to 34.5) kPa, and (34.5 to 68.9) kPa. With an automatic switching valve-manifold, the system was able to select the most relevant DP transducer based on the DP signal to be measured. This configuration avoided large relative uncertainties caused by using a large-range sensor to measure a small differential pressure signal. The system further included a pressure standard and a water column to calibrate the DP transducers in-situ.

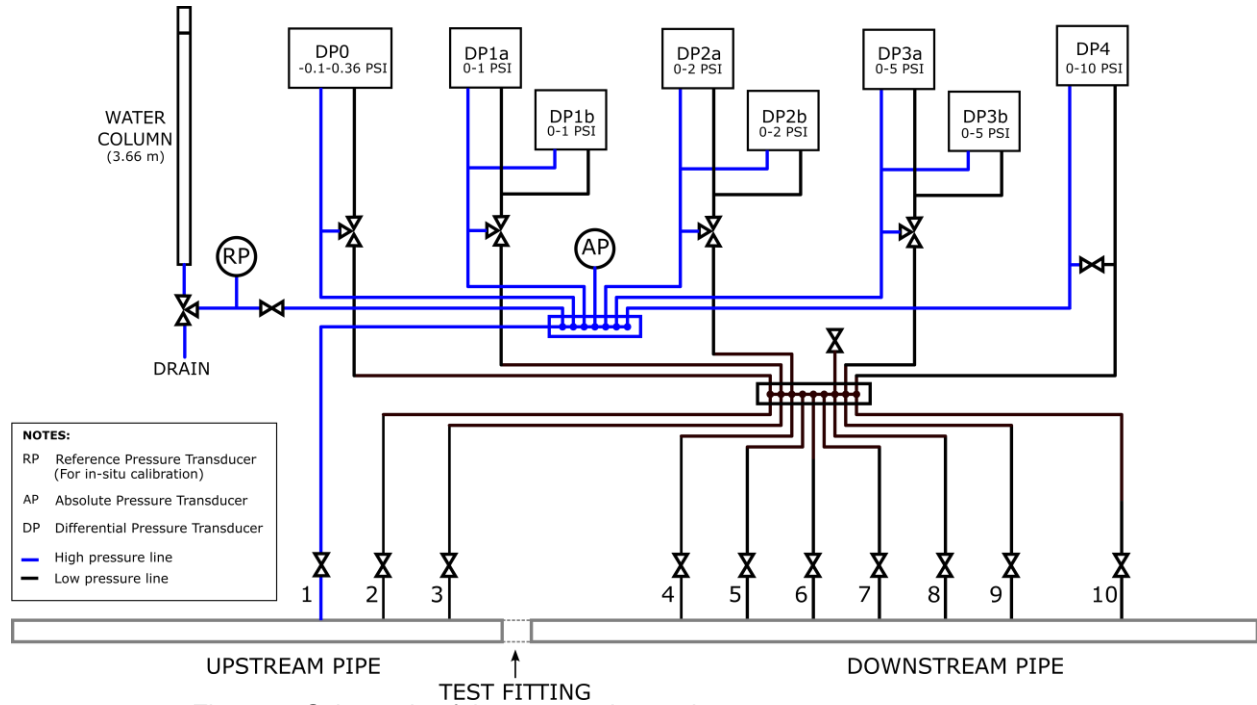


Figure 2. Schematic of the test section and pressure measurement system.

The measured static pressures of the ten tapping locations along the pipe were used to determine the upstream and downstream hydraulic grade lines using linear regression, which can be expressed by:

$$P_1(z) = k_1 z + P_{t,1} \quad (1)$$

$$P_2(z) = k_2 z + P_{t,2} \quad (2)$$

where  $P$  is the static pressure in kPa,  $z$  is the streamwise location in m,  $k$  is the slope [kPa/m],  $P_t$  is the intercept (i.e., static pressure at  $z = 0$ , which is where the fitting is located), and subscripts 1 and 2 represent upstream and downstream, respectively.

The pressure loss due to the fitting ( $\Delta P_L$ ) was calculated by the difference between the intercepts of the upstream and downstream hydraulic grade lines, i.e.:

$$\Delta P_L = P_{t,1} - P_{t,2} \quad (3)$$

The measured pressure loss was reduced to the dimensionless pressure loss coefficient,  $K_L$ :

$$K_L = \frac{2\Delta P_L}{\rho V^2} \quad (4)$$

where  $\rho$  is the water density,  $V$  is the average flow velocity derived from the mass flow rate ( $\dot{m}$ ):

$$V = \frac{4\dot{m}}{\rho\pi D^2} \quad (5)$$

The pressure loss of a fully-developed flow in a straight pipe can be described by the Darcy–Weisbach equation:

$$\Delta P = f \frac{\Delta z}{D} \frac{\rho V^2}{2} \quad (6)$$

where  $f$  is the friction factor, and  $D$  is the pipe diameter. Thus, the friction factor in the upstream or downstream straight pipe can be calculated from the slope of its hydraulic grade line:

$$f = \left(\frac{\Delta P}{\Delta z}\right) \frac{2D}{\rho V^2} = \frac{2kD}{\rho V^2} \quad (7)$$

By comparing the friction factor calculated from the upstream and downstream hydraulic grade lines, we were able to check if the flow was fully developed.

The pressure loss due to a fitting can also be expressed in term of the equivalent length,  $L_{eq}$ , defined as:

$$L_{eq} = \frac{D}{f} K_L \quad (8)$$

### 3. Test Fittings

An elbow and a coupling were tested in this study. Both fittings are made of copper, push-to-connect type, and have a nominal tube size (NTS) of  $\frac{3}{4}$ . Push-to-connect fittings were chosen for their ease of disconnection without cutting the pipes, allowing the test pipes to be reused. Figure 3 shows their dimensions, provided by the manufacturer. The plastic inserts that are originally included in both fittings were removed following the manufacturer’s installation instructions, as they are only used for plastic pipe installations. Upon installation, the test copper tube was inserted into each fitting to a depth of 28.78 mm.

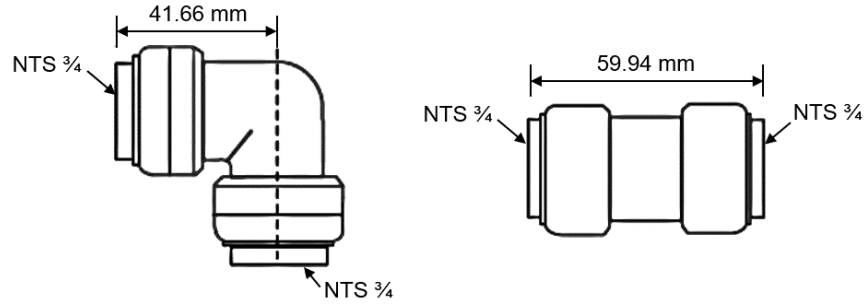


Figure 3. Dimensions of the test elbow and coupling

#### 4. Calculation of Measurement Uncertainty

The measurement uncertainties were calculated following the guidelines for evaluating and expressing uncertainty provided in NIST TN 1297 [9]. The detailed procedure is presented in the following sub-sections. Unless otherwise noted, the standard uncertainty of a quantity is denoted as  $u$ , and the expanded uncertainty is denoted as  $U$ , which is evaluated for a 95 % confidence interval.

##### 4.1. Uncertainty of Primary Measurements

A primary measurement is defined as the measurement taken directly from one or multiple identical instruments. Table 2 lists the primary measurements involved in this study along with their uncertainties. The evaluation procedure was as follows.

For any primary measurement quantity  $x$ , the uncertainty of the primary measurement ( $u$ ) was considered to have two components due to random and systematic errors, denoted as  $u_A$  and  $u_B$ , respectively:

$$u_x = \sqrt{u_{x,A}^2 + u_{x,B}^2} \quad (9)$$

The random component ( $u_A$ ) was evaluated statistically from the samples (i.e., Type A uncertainty evaluation):

$$u_{x,A} = \frac{s_x}{\sqrt{N_x}} \quad (10)$$

where  $s_x$  is the standard deviation of the measurement quantity among the samples;  $N_x$  is the number of samples.

The systematic component ( $u_{B,x}$ ) was evaluated by a non-statistical analysis (i.e., Type B uncertainty evaluation) — it was evaluated from the calibration information, either done in-house or provided by the manufacturer.

In our tests, each measurement was taken from a large number of samples ( $> 10^6$ ), leading to  $u_A \approx 0$  and  $u \approx u_B$ , meaning the combined uncertainty  $u$  was overridden by the uncertainty due to systematic errors. Thus, the uncertainties listed in Table 2 are essentially the uncertainties evaluated by the calibration, which were discussed in detail in [8].

Not mentioned in [8] is the fitting diameter measurement, which was done using a vernier caliper. The manufacturer states that the maximum permissible error (MPE) of the caliper is  $\pm 0.03 \text{ mm}^1$ . Assuming a rectangular error distribution, the standard uncertainty was then calculated as:  $\frac{0.03 \text{ mm}}{\sqrt{3}} = 0.0173 \text{ mm}$ .

The expanded uncertainty of the primary measurement ( $U$ ) was calculated by:

$$U_x = k_x \cdot u_x \quad (11)$$

where  $k_x$  is the coverage factor and was set to  $k_x = 2$  because  $N_x \gg 30$ .

Table 2. Uncertainties of primary measurements

Quantity	Symbol	Standard Uncertainty, $u$	Instrument
Mass flow rate	$\dot{m}$	$(0.707 \times 0.05 \% \times \dot{m}) \text{ kg/s}$ , for $\dot{m} \geq 0.264 \text{ kg/s}$ or $0.707 \times 0.95 \text{ kg/h}$ , for $\dot{m} \geq 0.264 \text{ kg/s}$	Two Coriolis meters
Density	$\rho$	$0.707 \text{ kg/m}^3$	Two Coriolis meters
Temperature	$T$	$(0.15 + 0.002 \times T) \text{ }^\circ\text{C}$	Two RTDs
Diameter	$D$	$0.0173 \text{ mm}$	Vernier caliper
Pressure*	$P$	$0.8 \text{ Pa}$	DP0
		$6.9 \text{ Pa}$	DP2b
		$12.5 \text{ Pa}$	DP3a and DP3b
* The DP transducers DP1a, DP1b, and DP2a were broken at the time of measurements and therefore not included here. The static pressure was measured using the rest of the DP transducers.			

## 4.2. Uncertainty of Pressure Loss

The standard uncertainty of the pressure loss,  $u_{\Delta P_{L,t}}$ , was calculated by

$$u_{\Delta P_L} = \sqrt{u_{P_{t,1}}^2 + u_{P_{t,2}}^2} \quad (12)$$

The uncertainty of  $P_{t,1}$  and  $P_{t,2}$  were calculated by

$$u_{P_{t,i}} = \sqrt{u_{\text{fit},i}^2 + u_p^2} \quad (13)$$

where  $i = 1$  (upstream) or  $2$  (downstream);  $u_{\text{fit}}$  is the standard deviation of the intercept obtained from the linear regression;  $u_p$  is evaluated by the maximum of the standard

<sup>1</sup> Based on the scale shift error (or S error), which applies to measurements using any measuring faces on the caliper other than the outside measuring faces, such as inside, step, and depth measurements.

uncertainties of the DP transducer used in the upstream or downstream measurements. For example, for a downstream measurement that involved using DP0 and DP2b, the  $u_p$  would be evaluated by the standard uncertainty of DP2, which was 6.9 Pa.

The expanded uncertainty,  $U_{\Delta P_L}$ , was calculated by

$$U_{\Delta P_L} = k_{\Delta P_L} \cdot u_{\Delta P_L} \quad (14)$$

where  $k_{\Delta P_L}$  is the coverage factor for 95 % confidence interval, evaluated by the student's t-distribution based on the degree of freedom associated with  $u_{\Delta P_L}$ , which was denoted as  $\nu_{\Delta P_L}$ .

$\nu_{\Delta P_L}$  was evaluated using the Welch-Satterthwaite formula:

$$\nu_{\Delta P_L} = \frac{u_{\Delta P_L}^4}{\frac{u_{P_{t,1}}^4}{\nu_{P_{t,1}}} + \frac{u_{P_{t,2}}^4}{\nu_{P_{t,2}}}} \quad (15)$$

$$\nu_{P_{t,1}} = \frac{u_{P_{t,1}}^4}{\frac{u_{\text{fit},1}^4}{\nu_{\text{fit},1}} + \frac{u_P^4}{\nu_P}} \quad (16)$$

$$\nu_{P_{t,2}} = \frac{u_{P_{t,2}}^4}{\frac{u_{\text{fit},2}^4}{\nu_{\text{fit},2}} + \frac{u_P^4}{\nu_P}} \quad (17)$$

The degree of freedom for a linear fit was calculated as follows:

$$\nu_{\text{fit},i} = N_i - 2 \quad (18)$$

where  $N_i$  is the number data points (i.e., pressure measurements) used for fitting. Here,  $N_1 = 3$  and  $N_2 = 7$ , yielding  $\nu_{\text{fit},1} = 1$  and  $\nu_{\text{fit},2} = 5$ .

### 4.3. Uncertainty of Velocity

The combined standard uncertainty of the velocity was calculated using the uncertainty propagation based on Eq. (5).

$$u_V = \sqrt{\left(\frac{\partial V}{\partial \dot{m}}\right)^2 u_{\dot{m}}^2 + \left(\frac{\partial V}{\partial \rho}\right)^2 u_{\rho}^2 + \left(\frac{4}{\rho \pi D^3}\right)^2 u_D^2} \quad (19)$$

$$\frac{\partial V}{\partial \dot{m}} = \frac{4}{\rho \pi D^2} \quad (20)$$

$$\frac{\partial V}{\partial \rho} = -\frac{4}{\rho^2 \pi D^2} \quad (21)$$

$$\frac{\partial V}{\partial D} = -\frac{4}{\rho \pi D^3} \quad (22)$$

The expanded uncertainty was evaluated by

$$U = k_V \cdot u_V \quad (23)$$

where the coverage factor was estimated as  $k_V = 2$ .

#### 4.4. Uncertainties of Pressure Loss Coefficient, $K_L$

Another factor that contributes to the large uncertainties is the low degree of freedom. Because it only has three pressure locations and the regression has two fitting constants, the degree of freedom associated with  $P_{t1}$ ,  $\nu_{P_{t1}}$ , is  $3 - 2 = 1$ , and the corresponding coverage factor (for 95 % confidence interval),  $k_{P_{t1}}$ , is 12. In comparison, the degree of freedom associated with  $P_{t2}$ ,  $\nu_{P_{t2}}$ , is  $7 - 2 = 5$ , and the corresponding coverage factor (for 95 % confidence interval),  $k_{P_{t2}}$ , is 2.7.

$$U_{K_L} = \sqrt{\left(\frac{\partial K_L}{\partial \Delta P_L}\right)^2 U_{\Delta P_L}^2 + \left(\frac{\partial K_L}{\partial \rho}\right)^2 U_{\rho}^2 + \left(\frac{\partial K_L}{\partial V}\right)^2 U_V^2} \quad (24)$$

$$\frac{\partial K_L}{\partial \Delta P_L} = \frac{2}{\rho V^2} \quad (25)$$

$$\frac{\partial K_L}{\partial \rho} = -\frac{2\Delta P_L}{\rho^2 V^2} \quad (26)$$

$$\frac{\partial K_L}{\partial V} = -\frac{4\Delta P_L}{\rho V^3} \quad (27)$$

Rearranging the above equations yields:

$$U_{K_L} = \sqrt{\left(\frac{2}{\rho V^2}\right)^2 U_{\Delta P_L}^2 + \left[\left(\frac{2\Delta P_L}{\rho^2 V^2}\right)^2 + \left(\frac{4\Delta P_L}{\rho V^3}\right)^2 \left(\frac{4}{\rho^2 \pi D^2}\right)^2\right] U_{\rho}^2 + \left(\frac{4\Delta P_L}{\rho V^3}\right)^2 \left(\frac{4}{\rho \pi D^2}\right)^2 U_{\dot{m}}^2 + \left(\frac{4\Delta P_L}{\rho V^3}\right)^2 \left(\frac{4}{\rho \pi D^3}\right)^2 U_D^2} \quad (28)$$

Note that there might be other contributors to the combined uncertainty of  $K_L$ . For example, if the pressure measurements were not done in the fully-developed regime, an error would be introduced to the determination of the pressure loss. This error was not accounted for in our study because our measurements seemed to remain in fully developed regime, as indicated by the friction factors measured at the upstream and downstream locations that were within  $\pm 2\%$ .

## 5. Measurement Data and Analysis

### 5.1. Elbow

Pressure losses in the push-to-connect elbow were measured from approximately 0.6 m/s to 4.6 m/s (i.e., 2 ft/s to 15 ft/s) and repeated three times on different days. Figure 4 shows the pressure loss coefficients ( $K_L$ ) measured in three independent tests (i.e., Test 1, Test 2, and Test 3). The error bars represent the expanded uncertainty of  $K_L$  for 95 % confidence interval. The measurements appear to be quite repeatable among the three tests. The measurements exhibit larger scatter in  $Re < 40000$ , which is mainly because of the increased uncertainty in pressure measurement at small pressures (discussed below). The uncertainty tends to be smaller at higher  $Re$ . For  $Re > 40000$ , the expanded uncertainties of  $K_L$  are within 0.03 (or 3 % of the mean value), except for two data points with much higher uncertainties that might be caused by unstable flow during the measurement. Tabulated measurement data and the associated uncertainties are provided in Appendix A.

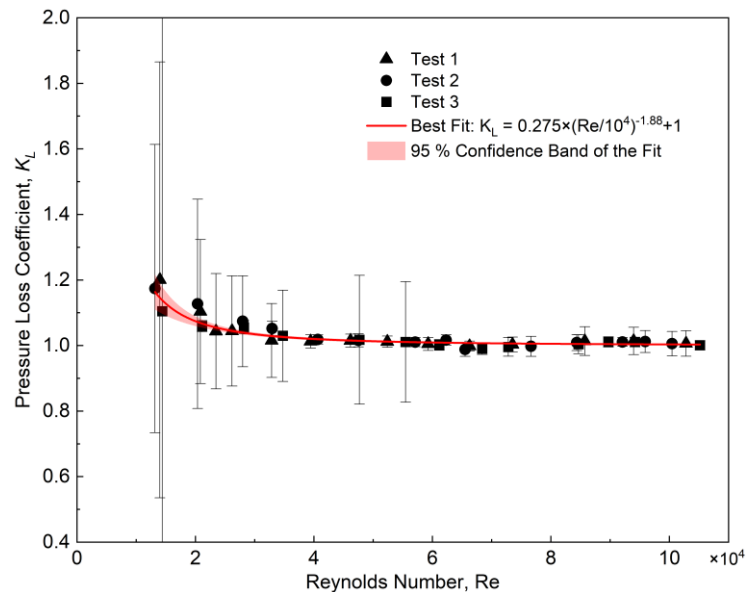


Figure 4. Pressure loss coefficient of elbow as a function of  $Re$

Figure 4 shows a clear trend of  $K_L$  that first decreases with the increasing  $Re$  and then plateaus when  $Re$  exceeds 40000. This trend agrees with several existing works in the literature as follows. The weakening effect of  $Re$  on  $K_L$  at high  $Re$  can be explained by the dominance of inertial effects. As the  $Re$  increases, inertia effects prevail over frictional effects, and the former cause flow separation and secondary flows, which both lead to pressure losses. Since inertia is

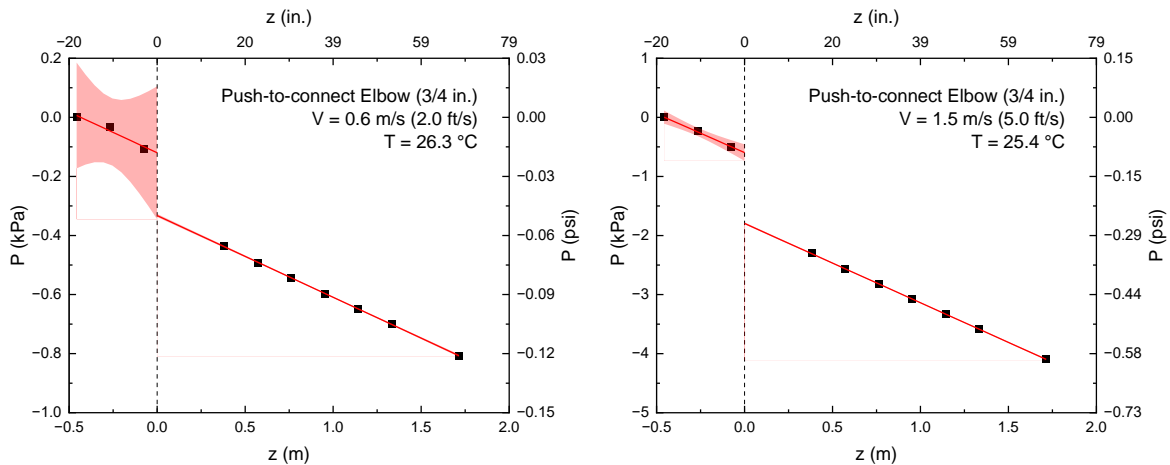
related to the dynamic pressure  $\frac{1}{2}\rho V^2$ , when it dominates the flow the pressure loss will tend to be proportional to the dynamic pressure, which translates to a constant  $K_L$ .

The  $K_L$  data in Figure 4 were correlated using weighted, non-linear regression, with weights calculated as  $1/U_{K_L}^2$ , where  $U_{K_L}$  is the expanded uncertainty of  $K_L$ . The best-fit equation is as follows:

$$K_L = 0.275 \times \left(\frac{\text{Re}}{10^4}\right)^{-1.88} + 1.0, \quad 14000 < \text{Re} < 105000 \quad (29)$$

Equation (29) suggests that  $K_L$  asymptotically approaches 1.0 as Re approaches infinity. In comparison, Al-Tameemi and Ricco [10] found that the asymptote for a sharp-angled miter elbow was 0.9. Considering the geometric variations, our measurements are in reasonable agreement with the measurements reported in the literature.

The major contributors to the uncertainty of  $K_L$  are the measured pressure losses, particularly  $P_{t,1}$  and  $P_{t,2}$ , which are calculated from the measured pressure distribution. Figure 5 shows the measured pressure distributions for three flow velocities from Test 3. The shaded band represents the 95 % confidence interval of the curve fits. At  $z = 0$ , the half-width of the band is equal to the standard deviation of the intercept, i.e.,  $u_{\text{fit}}$  as in Eq. (12). In our tests,  $u_{P,i}$  is dominated by  $u_{\text{fit}}$ , because  $u_{\text{fit}}$  is generally much larger than the uncertainty of individual DP measurements,  $u_P$ . Thus, the band half-width at  $z = 0$  can be used to interpret the  $u_{P,1}$  or  $u_{P,2}$ . As shown in Figure 5, the uncertainty is much more significant at upstream locations compared to downstream locations, particularly at medium and low velocities. The main reason is that, because the upstream pressures are smaller than those downstream, the systematic error inherent in DP measurement would contribute more to the combined uncertainty and cause more significant variations. In addition, the upstream section has fewer pressure measurement locations, and hence a smaller degree of freedom (DOF) for the fit. The DOF for the upstream fit is 1, and the corresponding coverage factor is 12.7. The DOF for the downstream fit is 5, and the corresponding coverage factor is 2.6. Since the expanded uncertainty is  $U = ku$ , a difference in DOF between 1 to 5 would lead to a dramatic change in expanded uncertainty.



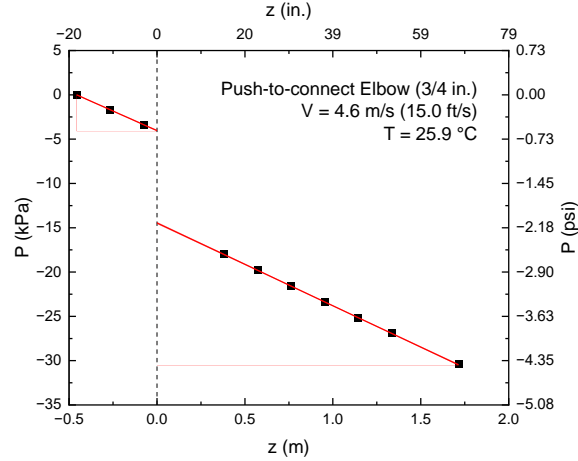


Figure 5. Pressure distribution for Test 3 of elbow at (a) 0.6 m/s (2 ft/s), (b) 1.5 m/s (5 ft/s), and (c) 4.6 m/s (15 ft/s).

The slope of the fitted hydraulic grade line is related to the friction factor of the straight pipe, as shown in Eq. (7). Ideally, the static pressures should be measured in the fully developed region to ensure the entire pressure loss due to the fitting is captured, and hence the friction factors measured in the upstream and downstream locations should be equal. Figure 6 shows the measured friction factor data in Test 3 for the straight pipes in the upstream and downstream of the elbow. The measurements are compared to the Colebrook correlation [11] where the surface roughness of the pipe,  $\varepsilon$ , is set to be 0.0015 mm [12]. As shown in Figure 6, the measured downstream friction factors agree very well with the Colebrook correlation (Eq. (30)) for the entire range of  $Re$ . While the uncertainty of the Colebrook equation is approximately within  $\pm 15\%$ , the deviation of our measurement and the Colebrook equation remains within  $\pm 2\%$ . The downstream and upstream measurements are within  $\pm 1\%$  for  $Re < 60000$ . From these results, it is reasonable to believe that the fluid flow in our tests was fully developed at the locations where the static pressures were measured.

$$\frac{1}{\sqrt{f}} = -2.0 \log \left( \frac{\varepsilon/D}{3.7} + \frac{2.51}{Re \sqrt{f}} \right) \quad (30)$$

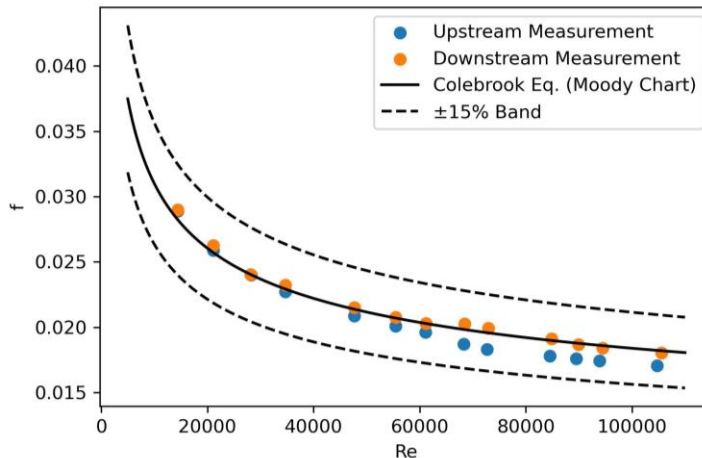


Figure 6. Friction factor ( $f$ ) of the straight pipes upstream and downstream of the elbow (Test 3).

Figure 7 shows the measured equivalent length ( $L_{eq}$ ) of the elbow, calculated using Eq. (8), where the friction factor is calculated by the Colebrook equation (Eq. (30)). A plot of equivalent length vs. volumetric flow rate in English units corresponding to Figure 7 is provided in Appendix B. The normalized equivalent length ( $L_{eq}/D$ ) is also shown, ranging from 40 to 55. The solid line in Figure 7 is computed using our correlation Eq. (29) along with Eqs. (8) and (30). The results clearly show that the equivalent length of the test elbow increases with increasing  $Re$ .

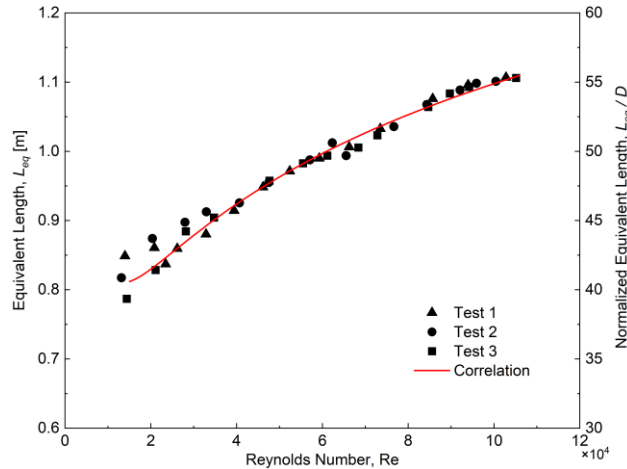


Figure 7. Equivalent length of the elbow as a function of  $Re$ .

## 5.2. Coupling

Figure 8 shows the pressure loss coefficient of the test coupling as a function of  $Re$ . Two data points were excluded because of the overly large uncertainties. No dependency of  $Re$  is observed. Thus, the data were averaged to obtain the mean value:  $K_L = 0.007$ . Figure 9 shows the equivalent length of the test coupling, calculated using the mean  $K_L$  along with Eqs. (8) and (30). The coupling's equivalent length is rather small, ranging from 0.17 in. to 0.30 in. for the test range of  $Re$ , which is just slightly larger than its actual internal length, i.e., 0.11 in. (see Figure 3). The difference between the actual internal length and the total equivalent length represents the pressure loss due to effects other than friction, which may include the local disturbance induced by O-rings and the gaps at the junction. Nonetheless, the results show that these non-friction effects are very small and may be neglected when sizing plumbing systems in practice. A plot of equivalent length vs. volumetric flow rate in English units corresponding to Figure 9 is provided in Appendix B.

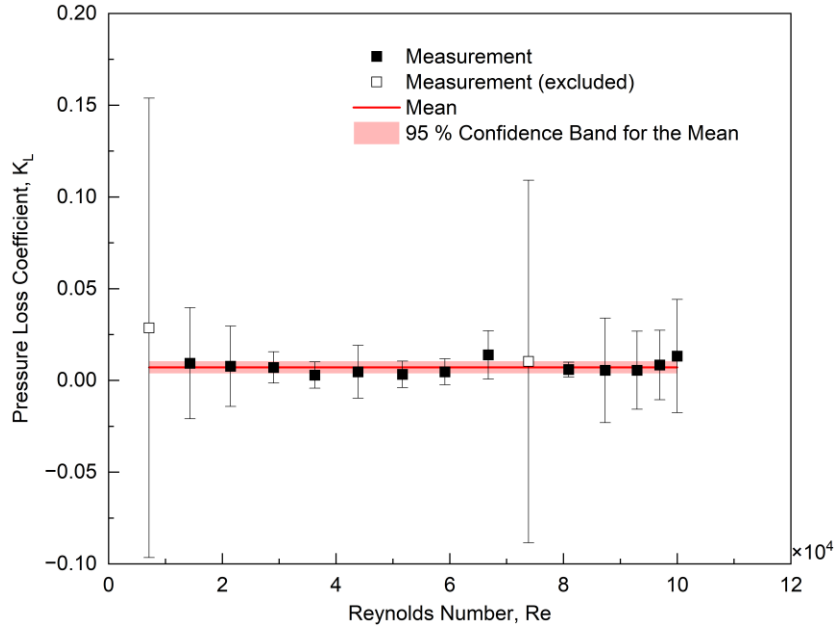


Figure 8. Pressure loss coefficient of the coupling as a function of Re

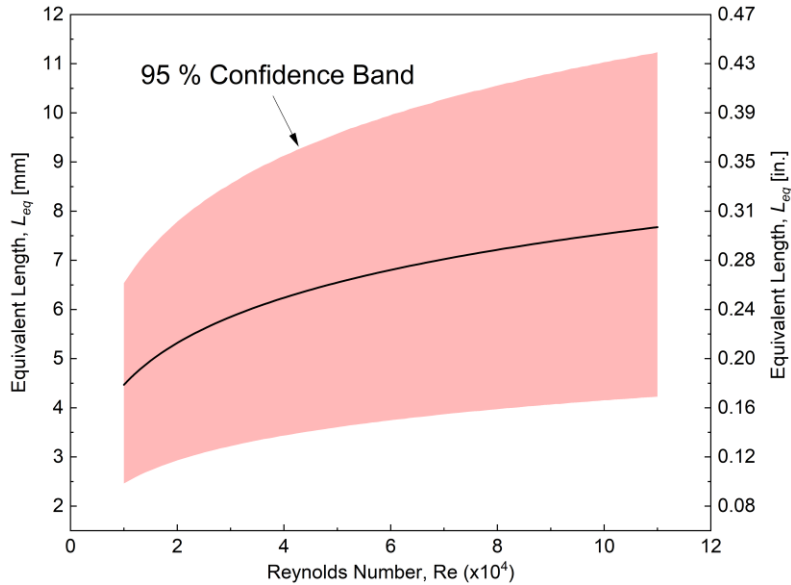


Figure 9. Equivalent length of the coupling as a function of Re calculated from the mean  $K_L$  of coupling

## 6. Conclusions

Pressure losses for copper push-to-connect elbow and coupling were measured over a Reynolds number ( $Re$ ) range of approximately  $10^4$  to  $10^5$ . The results show that the pressure loss coefficient ( $K_L$ ) of elbow decreases with increasing  $Re$  and stabilizes near 1.0 as  $Re$  exceeds 40,000, while the coupling maintains a nearly constant  $K_L$  across the entire range. These findings

suggest that current plumbing design practices, which often assume Re-independent  $K_L$ , can underestimate losses in fittings like elbows at low flowrates. Incorporating Re-dependent correlations can improve the sizing accuracy. In addition, the uncertainty of  $K_L$  tends to be larger at smaller Re. Regarding the pressure loss test method, the current setup had three pressure taps upstream and five downstream. We found that additional tapping locations upstream can reduce the uncertainty associated with the pressure loss measurement. Increasing the upstream tapping locations from three to five can result in a reduction of the expanded uncertainty of  $K_L$  by up to 75 %.

## References

- [1] National Academies of Sciences Engineering and Medicine (NASEM) (2019) *Management of Legionella in Water Systems* (National Academies Press, Washington, D.C.). <https://doi.org/10.17226/25474>
- [2] ASHRAE (2021) Chapter 22 - Pipe Design. *ASHRAE Handbook - Fundamentals*
- [3] Crane Co. (2013) *Flow of Fluids Through Valves, Fittings and Pipe. Technical Paper No. 410M Metric Version.*
- [4] Idelchik IE (2007) *Handbook of hydraulic resistance*, 4th Ed.
- [5] Hydraulic Institute (1990) *Hydraulic Institute Engineering Data Book*, 2nd Ed.
- [6] Miller DS (1990) *Internal flow systems*, 2nd Ed.
- [7] Lin L, Batista MD, Ferretti NM (2022) State-of-the-art review on measurement of pressure losses of fluid flow through pipe fittings. *NIST Technical Note 2206*. <https://doi.org/10.6028/NIST.TN.2206>
- [8] Lin L, Ferretti NM, Glaeser G (2024) Test facility for pressure losses in plumbing pipes and fittings. *NIST Technical Note 2294* <https://doi.org/10.6028/NIST.TN.2294>
- [9] Taylor BN, Kuyatt CE (1994) Guidelines for Evaluating and Expressing the Uncertainty of NIST Measurement Results. *NIST Technical Note 1297*.
- [10] Al-Tameemi WTM, Ricco P (2018) Pressure-Loss Coefficient of 90 deg Sharp-Angled Miter Elbows. *Journal of Fluids Engineering* 140(6):1–7. <https://doi.org/10.1115/1.4038986>
- [11] Colebrook CF (1939) Turbulent Flow in pipes, with particular reference to the transition region between the smooth and rough pipe laws. *Journal of the Institution of Civil Engineers* 11(4):133–156. <https://doi.org/10.1680/ijoti.1939.13150>
- [12] Çengel YA, Cimbala JM (2006) *Fluid Mechanics - Fundamentals and Applications* (McGraw-Hill).

## Appendix A. Test Data and Uncertainties

Table A1. Uncertainties of elbow pressure losses

$V$	$V$	Re	$P_{t,1}$	$u_{P_{t,1}}$	$v_{P_{t,1}}$	$P_{t,2}$	$u_{P_{t,2}}$	$v_{P_{t,2}}$	$\Delta P_L$	$u_{\Delta P_L}$	$v_{\Delta P_L}$	$k_{\Delta P_L}$	$U_{\Delta P_L}$	$\frac{U_{\Delta P_L}}{\Delta P_L}$
m/s	ft/s	-	Pa	Pa	-	Pa	Pa	-	Pa	Pa	-	-	Pa	-
Test 1														
0.6	2.0	13980	-101.3	9.9	1.0	-329.9	1.3	12.5	228.6	10.0	1.0	12.7	126.6	55%
0.9	3.0	20836	-230.7	7.2	1.0	-696.4	1.4	11.4	465.7	7.3	1.1	12.7	92.5	20%
1.1	3.6	23463	-358.2	7.3	1.0	-982.1	3.9	5.4	624.0	8.3	1.7	12.7	105.0	17%
1.2	4.0	26172	-425.8	8.8	1.0	-1201.5	4.4	5.4	775.7	9.8	1.6	12.7	124.8	16%
1.5	5.0	32857	-623.6	9.5	1.0	-1807.7	4.0	5.4	1184.0	10.3	1.4	12.7	131.0	11%
1.8	6.0	39434	-838.2	7.7	1.0	-2531.2	8.8	5.1	1693.0	11.6	4.1	2.8	32.3	2%
2.1	7.0	46156	-1081.1	6.1	1.0	-3392.2	15.7	5.0	2311.1	16.8	6.0	2.6	43.3	2%
2.4	8.0	52382	-1369.2	5.4	1.0	-4372.3	18.1	5.0	3003.1	18.9	5.7	2.6	48.6	2%
2.7	9.0	59284	-1687.7	13.3	1.0	-5469.2	26.2	5.8	3781.6	29.4	6.6	2.4	71.9	2%
3.1	10.0	66259	-1994.1	1.0	6.5	-6625.9	26.7	5.7	4631.8	26.7	5.8	2.6	68.6	1%
3.4	11.0	73502	-2349.6	3.0	1.2	-7981.1	48.6	5.2	5631.5	48.7	5.2	2.6	125.2	2%
4.0	13.0	85711	-3152.8	63.4	1.0	-11084.6	48.2	6.1	7931.8	79.7	2.4	4.3	342.8	4%
4.3	14.0	93962	-3580.8	70.4	1.0	-12803.0	52.2	5.9	9222.2	87.6	2.3	4.3	377.1	4%
4.6	15.0	102798	-4031.8	69.9	1.0	-14537.5	63.1	5.6	10505.7	94.2	2.9	4.3	405.1	4%
Test 2														
0.6	2.0	13161	-107.2	6.1	1.0	-323.9	1.9	7.3	216.7	6.4	1.3	12.7	81.1	37%
0.9	3.0	20356	-222.5	10.4	1.0	-694.5	1.6	8.6	472.0	10.5	1.1	12.7	133.5	28%
1.2	4.0	27971	-382.7	7.7	1.0	-1183.3	2.5	6.3	800.6	8.1	1.2	12.7	103.2	13%
1.5	5.0	32938	-585.6	5.5	1.0	-1804.1	4.9	5.3	1218.5	7.4	3.0	3.2	23.6	2%
1.8	6.0	40647	-818.6	3.7	1.1	-2517.0	9.3	24.3	1698.4	10.0	21.1	2.1	20.9	1%
2.1	7.0	47487	-1076.8	10.4	1.0	-3391.8	14.6	8.3	2314.9	18.0	6.0	2.4	43.9	2%
2.4	8.0	57085	-1339.4	8.7	1.0	-4347.9	14.5	8.3	3008.5	16.9	7.5	2.4	40.0	1%
2.7	9.0	62304	-1626.6	6.3	1.0	-5449.9	22.1	6.1	3823.3	23.0	6.9	2.4	56.3	1%
3.0	10.0	65524	-2035.1	18.6	1.0	-6609.0	34.9	5.4	4573.9	39.6	6.2	2.4	96.8	2%
3.4	11.0	76653	-2334.8	6.7	1.0	-7943.1	66.0	5.1	5608.4	66.3	5.2	2.6	170.4	3%
3.7	12.0	84354	-2704.0	4.7	1.1	-9478.2	62.1	5.4	6774.1	62.3	5.5	2.6	160.0	2%
4.0	13.0	92085	-3102.9	2.4	1.3	-11027.5	40.8	6.1	7924.6	40.8	6.1	2.4	99.9	1%
4.3	14.0	95918	-3575.5	53.6	1.0	-12773.5	46.2	5.8	9198.1	70.8	2.8	4.3	304.4	3%
4.6	15.0	100450	-4094.4	72.5	1.0	-14605.4	53.8	5.6	10511.1	90.3	2.3	4.3	388.5	4%
Test 3														
0.6	2.0	14388	-120	17.7	1.0	-332.5	2.2	6.6	212.4	17.9	1.0	12.7	227.0	107%
0.9	3.0	21099	-246	1.1	5.2	-689.5	1.9	7.4	443.5	2.2	11.2	2.2	4.8	1%
1.2	4.0	28170	-404	1.9	1.5	-1189.1	5.1	5.3	784.6	5.5	6.4	2.4	13.4	2%
1.5	5.0	34727	-596	11.1	1.0	-1795.4	6.3	5.2	1198.6	12.7	1.7	12.7	162.0	14%
2.1	7.0	47666	-1064	33.7	1.0	-3376.8	9.8	5.1	2311.9	35.1	1.2	12.7	446.3	19%
2.4	8.0	55475	-1338	41.0	1.0	-4335.8	12.9	5.0	2997.5	43.0	1.2	12.7	545.8	18%
2.7	9.0	61148	-1672.5	13.7	1.0	-5438.5	18.5	6.7	3766.0	23.1	5.4	2.6	59.3	2%
3.1	10.0	68385	-1967.7	9.7	1.0	-6563.7	30.9	5.5	4595.9	32.4	6.3	2.4	79.4	2%
3.3	11.0	72809	-2336.0	16.4	1.0	-7907.4	58.8	5.1	5571.4	61.0	5.8	2.6	156.9	3%
3.7	12.0	84665	-2692.8	7.4	1.0	-9388.2	73.9	5.1	6695.4	74.2	5.2	2.6	190.8	3%
4.0	13.0	89705	-3139.2	0.8	2855.0	-11070.9	46.5	5.8	7931.8	46.6	5.8	2.6	119.7	2%
4.3	14.0	94183	-3607.9	0.8	209.7	-12811.9	50.3	5.7	9204.0	50.3	5.7	2.6	129.3	1%
4.6	15.0	105152	-4037.0	6.2	1.0	-14466.6	53.4	5.6	10429.6	53.7	5.7	2.6	138.1	1%

Table A2. Uncertainties of the elbow's pressure loss coefficient and its components

V	V	Re	$\Delta P_L$	$U_{\Delta P_L}$	$\rho$	$U_\rho$	$\dot{m}$	$U_{\dot{m}}$	D	$U_D$	$K_L$	$U_{K_L}$	$\frac{U_{K_L}}{K_L}$	Contribution to $U_{K_L}$				
														$\Delta P_L$	$\rho$	$\dot{m}$	D	
m/s	ft/s	1	Pa	Pa	kg/m <sup>3</sup>	1	kg/s	1	m	m	1	1	1	1	1	1	1	1
Test 1																		
0.6	2.0	13980	228.6	126.6	996.8	1.4	0.197	3.7E-04	0.02011	3.5E-05	1.20	0.67	55%	100%	0%	0%	0%	
0.9	3.0	20836	465.7	92.5	996.7	1.4	0.290	2.0E-04	0.02011	3.5E-05	1.10	0.22	20%	100%	0%	0%	0%	
1.1	3.6	23463	624.0	105.0	997.4	1.4	0.386	2.7E-04	0.02011	3.5E-05	1.04	0.18	17%	100%	0%	0%	0%	
1.2	4.0	26172	775.7	124.8	997.4	1.4	0.484	3.4E-04	0.02011	3.5E-05	1.04	0.17	16%	100%	0%	0%	0%	
1.5	5.0	32857	1184.0	131.0	997.4	1.4	0.676	4.7E-04	0.02011	3.5E-05	1.02	0.11	11%	100%	0%	0%	0%	
1.8	6.0	39434	1693.0	32.3	997.3	1.4	0.772	5.3E-04	0.02011	3.5E-05	1.01	0.02	2%	90%	0%	1%	9%	
2.1	7.0	46156	2311.1	43.3	997.3	1.4	0.869	6.0E-04	0.02011	3.5E-05	1.01	0.02	2%	92%	1%	1%	7%	
2.4	8.0	52382	3003.1	48.6	997.4	1.4	0.966	6.7E-04	0.02011	3.5E-05	1.01	0.02	2%	91%	1%	1%	7%	
2.7	9.0	59284	3781.6	71.9	997.3	1.4	1.061	7.3E-04	0.02011	3.5E-05	1.00	0.02	2%	95%	1%	1%	4%	
3.1	10.0	66259	4631.8	68.6	997.3	1.4	1.158	8.0E-04	0.02011	3.5E-05	1.00	0.02	2%	93%	1%	1%	5%	
3.4	11.0	73502	5631.5	125.2	997.2	1.4	1.256	8.7E-04	0.02011	3.5E-05	1.00	0.02	2%	97%	0%	1%	2%	
4.0	13.0	85711	7931.8	342.8	997.3	1.4	1.353	9.4E-04	0.02011	3.5E-05	1.01	0.04	4%	99%	0%	0%	0%	
4.3	14.0	93962	9222.2	377.1	997.2	1.4	1.447	1.0E-03	0.02011	3.5E-05	1.01	0.04	4%	99%	0%	0%	0%	
4.6	15.0	102798	10505.7	405.1	996.9	1.4	1.447	1.0E-03	0.02011	3.5E-05	1.01	0.04	4%	99%	0%	0%	0%	
Test 2																		
0.6	2.0	13161	216.7	81.1	997.3	1.4	0.193	3.7E-04	0.02011	3.5E-05	1.17	0.44	37%	100%	0%	0%	0%	
0.9	3.0	20356	472.0	133.5	997.0	1.4	0.290	2.0E-04	0.02011	3.5E-05	1.13	0.32	28%	100%	0%	0%	0%	
1.2	4.0	27971	800.6	103.2	996.6	1.4	0.387	2.7E-04	0.02011	3.5E-05	1.07	0.14	13%	100%	0%	0%	0%	
1.5	5.0	32938	1218.5	23.6	997.3	1.4	0.483	3.3E-04	0.02011	3.5E-05	1.05	0.02	2%	87%	0%	0%	12%	
1.8	6.0	40647	1698.4	20.9	997.0	1.4	0.579	4.0E-04	0.02011	3.5E-05	1.02	0.01	1%	79%	1%	1%	19%	
2.1	7.0	47487	2314.9	43.9	997.0	1.4	0.677	4.7E-04	0.02011	3.5E-05	1.02	0.02	2%	92%	0%	0%	7%	
2.4	8.0	57085	3008.5	40.0	996.4	1.4	0.774	5.4E-04	0.02011	3.5E-05	1.01	0.01	1%	88%	1%	1%	10%	
2.7	9.0	62304	3823.3	56.3	996.8	1.4	0.870	6.0E-04	0.02011	3.5E-05	1.02	0.02	2%	92%	1%	1%	7%	
3.0	10.0	65524	4573.9	96.8	997.4	1.4	0.965	6.7E-04	0.02011	3.5E-05	0.99	0.02	2%	96%	0%	0%	3%	
3.4	11.0	76653	5608.4	170.4	996.7	1.4	1.063	7.4E-04	0.02011	3.5E-05	1.00	0.03	3%	98%	0%	0%	1%	
3.7	12.0	84354	6774.1	160.0	996.6	1.4	1.162	8.1E-04	0.02011	3.5E-05	1.01	0.02	2%	98%	0%	0%	2%	
4.0	13.0	92085	7924.6	99.9	996.5	1.4	1.255	8.7E-04	0.02011	3.5E-05	1.01	0.01	1%	93%	1%	1%	4%	
4.3	14.0	95918	9198.1	304.4	996.9	1.4	1.352	9.4E-04	0.02011	3.5E-05	1.01	0.03	3%	99%	0%	0%	1%	
4.6	15.0	100450	10511.1	388.5	997.2	1.4	1.450	1.0E-03	0.02011	3.5E-05	1.01	0.04	4%	99%	0%	0%	0%	
Test 3																		
0.6	2.0	14388	212.4	227.0	996.8	1.4	0.197	3.7E-04	0.02011	3.5E-05	1.10	1.18	107%	100%	0%	0%	0%	
0.9	3.0	21099	443.5	4.8	996.7	1.4	0.290	2.0E-04	0.02011	3.5E-05	1.06	0.02	2%	45%	1%	1%	54%	
1.2	4.0	28170	784.6	13.4	997.4	1.4	0.386	2.7E-04	0.02011	3.5E-05	1.06	0.02	2%	78%	1%	1%	21%	
1.5	5.0	34727	1198.6	162.0	997.4	1.4	0.484	3.4E-04	0.02011	3.5E-05	1.03	0.14	14%	100%	0%	0%	0%	
2.1	7.0	47666	2311.9	446.3	997.4	1.4	0.676	4.7E-04	0.02011	3.5E-05	1.02	0.20	19%	100%	0%	0%	0%	
2.4	8.0	55475	2997.5	545.8	997.3	1.4	0.772	5.3E-04	0.02011	3.5E-05	1.01	0.18	18%	100%	0%	0%	0%	
2.7	9.0	61148	3766.0	59.3	997.3	1.4	0.869	6.0E-04	0.02011	3.5E-05	1.00	0.02	2%	93%	1%	1%	6%	
3.1	10.0	68385	4595.9	79.4	997.4	1.4	0.966	6.7E-04	0.02011	3.5E-05	0.99	0.02	2%	95%	1%	1%	4%	
3.3	11.0	72809	5571.4	156.9	997.3	1.4	1.061	7.3E-04	0.02011	3.5E-05	1.00	0.03	3%	98%	0%	0%	1%	
3.7	12.0	84665	6695.4	190.8	997.3	1.4	1.158	8.0E-04	0.02011	3.5E-05	1.00	0.03	3%	98%	0%	0%	1%	
4.0	13.0	89705	7931.8	119.7	997.2	1.4	1.256	8.7E-04	0.02011	3.5E-05	1.01	0.02	2%	95%	1%	1%	3%	
4.3	14.0	94183	9204.0	129.3	997.3	1.4	1.353	9.4E-04	0.02011	3.5E-05	1.01	0.01	1%	95%	1%	1%	3%	
4.6	15.0	105152	10429.6	138.1	997.2	1.4	1.447	1.0E-03	0.02011	3.5E-05	1.00	0.01	1%	95%	1%	1%	3%	

Table A3. Uncertainties of coupling pressure losses

$V$	$V$	Re	$P_{t,1}$	$u_{P_{t,1}}$	$v_{P_{t,1}}$	$P_{t,2}$	$u_{P_{t,2}}$	$v_{P_{t,2}}$	$\Delta P_L$	$u_{\Delta P_L}$	$v_{\Delta P_L}$	$k_{\Delta P_L}$	$U_{\Delta P_L}$	$\frac{U_{\Delta P_L}}{\Delta P_L}$
m/s	ft/s	1	Pa	Pa	1	Pa	Pa	1	Pa	Pa	1	1	Pa	1
0.3	1.0	7112	-33.0	1.5	1.9	-34.3	0.9	88.9	1.3	1.8	3.6	3.2	5.6	437%
0.6	2.0	14307	-113.6	1.5	2.0	-115.3	0.8	541.8	1.7	1.7	3.5	3.2	5.4	322%
0.9	2.9	21444	-228.3	1.8	1.6	-231.4	0.9	66.4	3.1	2.0	2.5	4.3	8.7	282%
1.2	3.9	29018	-382.0	1.7	1.6	-387.1	1.4	10.9	5.1	2.2	4.3	2.8	6.1	120%
1.5	4.9	36252	-557.7	1.5	1.9	-561.0	3.0	5.8	3.3	3.4	7.6	2.4	7.9	244%
1.8	5.9	43868	-769.7	4.3	1.1	-777.3	3.3	5.6	7.6	5.4	2.6	4.3	23.2	304%
2.1	6.9	51684	-1010.6	3.6	1.1	-1018.0	4.5	5.3	7.4	5.7	4.8	2.8	15.9	215%
2.4	7.9	59141	-1267.7	4.1	1.1	-1281.1	6.7	5.1	13.5	7.9	5.8	2.6	20.3	150%
2.7	8.9	66770	-1533.2	10.5	1.0	-1584.1	10.7	14.5	50.9	15.0	3.9	3.2	47.9	94%
3.0	9.8	73853	-1853.8	31.2	1.0	-1900.0	15.3	7.9	46.3	34.8	1.5	12.7	441.6	955%
3.3	10.8	80907	-2233.9	5.6	1.0	-2266.2	8.0	77.7	32.3	9.7	9.2	2.3	22.0	68%
3.6	11.8	87335	-2561.5	32.9	1.0	-2597.1	27.3	5.7	35.6	42.7	2.6	4.3	183.7	516%
3.9	12.8	92927	-2972.5	30.7	1.0	-3014.7	21.3	11.6	42.2	37.4	2.2	4.3	160.9	381%
4.2	13.8	96930	-3406.0	36.1	1.0	-3480.0	37.6	6.3	73.9	52.2	3.7	3.2	166.0	225%
4.5	14.7	99988	-3869.2	58.5	1.0	-4002.9	42.1	6.0	133.6	72.1	2.2	4.3	310.3	232%

Table A4. Uncertainties of the coupling's pressure loss coefficient and its components

$V$	$V$	Re	$\Delta P_L$	$U_{\Delta P_L}$	$\rho$	$U_\rho$	$\dot{m}$	$U_{\dot{m}}$	$D$	$U_D$	$K_L$	$U_{K_L}$	$\frac{U_{K_L}}{K_L}$	Contribution to $U_{K_L}$			
														$\Delta P_L$	$\rho$	$\dot{m}$	$D$
m/s	ft/s	1	Pa	Pa	kg/m <sup>3</sup>	1	kg/s	1	m	m	1	1	1	1	1	1	1
Test 1																	
0.3	1.0	7112	1.3	5.6	996.0	1.4	0.095	3.7E-04	0.02011	3.5E-05	0.029	0.125	437%	100%	0%	0%	0%
0.6	2.0	14307	1.7	5.4	995.9	1.4	0.190	1.3E-04	0.02011	3.5E-05	0.009	0.030	322%	100%	0%	0%	0%
0.9	2.9	21444	3.1	8.7	995.8	1.4	0.283	2.0E-04	0.02011	3.5E-05	0.008	0.022	282%	100%	0%	0%	0%
1.2	3.9	29018	5.1	6.1	995.7	1.4	0.380	2.6E-04	0.02011	3.5E-05	0.007	0.009	120%	100%	0%	0%	0%
1.5	4.9	36252	3.3	7.9	995.6	1.4	0.472	3.3E-04	0.02011	3.5E-05	0.003	0.007	244%	100%	0%	0%	0%
1.8	5.9	43868	7.6	23.2	995.6	1.4	0.568	3.9E-04	0.02011	3.5E-05	0.005	0.014	304%	100%	0%	0%	0%
2.1	6.9	51684	7.4	15.9	995.5	1.4	0.665	4.6E-04	0.02011	3.5E-05	0.003	0.007	215%	100%	0%	0%	0%
2.4	7.9	59141	13.5	20.3	995.5	1.4	0.758	5.3E-04	0.02011	3.5E-05	0.005	0.007	150%	100%	0%	0%	0%
2.7	8.9	66770	50.9	47.9	995.5	1.4	0.855	5.9E-04	0.02011	3.5E-05	0.014	0.013	94%	100%	0%	0%	0%
3.0	9.8	73853	46.3	441.6	995.5	1.4	0.947	6.6E-04	0.02011	3.5E-05	0.010	0.099	955%	100%	0%	0%	0%
3.3	10.8	80907	32.3	22.0	995.6	1.4	1.044	7.2E-04	0.02011	3.5E-05	0.006	0.004	68%	100%	0%	0%	0%
3.6	11.8	87335	35.6	183.7	995.8	1.4	1.139	7.9E-04	0.02011	3.5E-05	0.006	0.028	516%	100%	0%	0%	0%
3.9	12.8	92927	42.2	160.9	996.0	1.4	1.234	8.5E-04	0.02011	3.5E-05	0.006	0.021	381%	100%	0%	0%	0%
4.2	13.8	96930	73.9	166.0	996.4	1.4	1.327	9.2E-04	0.02011	3.5E-05	0.008	0.019	225%	100%	0%	0%	0%
4.5	14.7	99988	133.6	310.3	996.9	1.4	1.422	9.8E-04	0.02011	3.5E-05	0.013	0.031	232%	100%	0%	0%	0%

## Appendix B. Equivalent Length vs. Volumetric Flow Rate in English Units

